AIAA JOURNAL
Vol. 37, No. 9, September 1999

Multilayered Shell Theories Accounting for Layerwise Mixed Description, Part 2: Numerical Evaluations

Erasmo Carrera*
Politecnico di Torino, 10129 Turin, Italy

The mixed layerwise shell theories that are presented in the companion article (E. Carrera, "Multilayered Shell Theories Accounting for Layerwise Mixed Description, Part 1: Governing Equations" *AIAA Journal*, Vol. 37, No. 9, 1999, pp. 1107–1116) are evaluated here by solving several problems related to orthotropic cross-ply laminated, circular, cylindrical, and spherical shells subjected to static loadings for which closed-form solutions are given. Particular cases related to layerwise and equivalent single-layer models, based on classical displacement formulations, are evaluated for comparison purpose. A further comparison with three-dimensional elasticity exact solutions and to other higher-order shear deformations studies have been made. Results are given in the form of tables and diagrams. Approximations introduced by Donnell's shallow shell theories are evaluated for most of the problems. It has been concluded that the proposed mixed layerwise theories leads to a better description than the related analyses, which are based on displacement formulations. An excellent agreement, with respect to the exact solution, has been found for displacement and transverse stress components. These stresses have been herein calculated a priori. The importance of an adequate description of curvature terms related to the shell thickness to radii ratio *h/R* is also underlined. These effects have been contrasted by extensive use of fictitious interfaces in the conduced layerwise investigations.

I. Closed-Form Solutions for Shells Composed of Orthotropic Layers

THE author's paper[1] has presented the governing equations of multilayered shell according to mixed layerwise descriptions. The boundary value problem governed by Eqs. (16–17) and Eqs. (27–28) of Ref. 1, in the most general case of geometry, boundary conditions, and layouts, could be solved by only implementing approximated solution procedures. To assess the proposed models these equations are herein solved for a special case in which closed-form solutions are given. The particular case in which the material has the properties (as it is the case of cross-ply shells)

$$\tilde{C}_{16} = \tilde{C}_{26} = \tilde{C}_{36} = \tilde{C}_{45} = 0$$

has been considered, for which Navier-type closed-form solutions can be found by assuming the following harmonic forms for the applied loadings $\boldsymbol{p}^k = \{p^k_{\alpha_\tau}, p^k_{\beta_\tau}, p^k_{z_\tau}\}$ and unknown displacement $\boldsymbol{u}^k = \{u^k_{\alpha_\tau}, u^k_{\beta_\tau}, u^k_{z_\tau}\}$ and stress $\boldsymbol{\sigma}^k_n = \{\sigma^k_{\alpha z_\tau}, \sigma^k_{\beta z_\tau}, \sigma^k_{z z_\tau}\}$ variables in each k layer:

$$\left(u^k_{\alpha_\tau}, \sigma^k_{\alpha z_\tau}, p^k_{\alpha_\tau}\right) = \sum_{m,n} \left(U^k_\alpha, S^k_{\alpha z_\tau}, P^k_{\alpha_\tau}\right) \cos\frac{m\pi\alpha_k}{a_k} \sin\frac{n\pi\beta_k}{b_k}$$

$$k = 1, N_l$$

$$\left(u^k_{\beta_\tau}, \sigma^k_{\beta z_\tau}, p^k_{\beta_\tau}\right) = \sum_{m,n} \left(U^k_\beta, S^k_{\beta z_\tau}, P^k_{\beta_\tau}\right) \sin\frac{m\pi\alpha_k}{a_k} \cos\frac{n\pi\beta_k}{b_k}$$

$$\tau = t, b, r$$

$$\left(u^k_{z_\tau}, \sigma^k_{z z_\tau}, p^k_{z_\tau}\right) = \sum_{m,n} \left(U^k_z, S^k_{z z_\tau}, P^k_{z_\tau}\right) \sin\frac{m\pi\alpha_k}{a_k} \sin\frac{n\pi\beta_k}{b_k}$$

$$r = 2, N \quad (1)$$

where α_k, β_k, z_k are curvilinear coordinates of the orthogonal reference system that lie on the reference surface of the k-layer Ω_k. The a_k and b_k are the shell lengths in the α_k and β_k directions, respectively, whereas m and n are the correspondent wave numbers. Capital letters on the left-hand side denote correspondent maximum amplitudes. Further nomenclature can be read in Ref. 1. The assumed functions correspond to simply supported shells. Upon substitution of Eqs. (1) the governing equations assume the form of a linear system of algebraic equations. The explicit forms assumed by the k-layer arrays that were derived in Ref. 1 are not shown here for the sake of brevity. These could easily be derived from those in Eqs. (20–25) and Eqs. (30–31) of Ref. 1. Related multilayered arrays are then written by implementing the same assemblage procedure described in Sec. VII of Ref. 1. This procedure has been coded and the results are discussed in the next sections.

II. Implemented Analyses

A number of comparisons have been made to evaluate the performance of the proposed layerwise mixed theories with respect to exact three-dimensional solutions, as well as related analyses based on displacement formulations [of layerwise modal (LWM) and equivalent single-layer model (ESLM) type]. A compendium of the acronyms used to denote the theories has been given in Table 1. Continuous reference to these acronyms is made in the subsequent discussion. Those theories implemented in the present study are briefly outlined in this section. In a few cases the tables report results related to Donnell-type approximations and a suffix .Δ has been added to the acronyms to indicate this.

A. Layerwise Models

Two cases of mixed models of Sec. III of Ref. 1 have been considered. A linear expansion (M-l) in each k layer,

$$\boldsymbol{u}^k = F_t \boldsymbol{u}^k_t + F_b \boldsymbol{u}^k_b \qquad k = 1, 2, \ldots, N_l$$

$$\boldsymbol{\sigma}^k_{nM} = F_t \boldsymbol{\sigma}^k_{nt} + F_b \boldsymbol{\sigma}^k_{nb} \quad (2)$$

and a parabolic expansion (M-p),

$$\boldsymbol{u}^k = F_t \boldsymbol{u}^k_t + F_b \boldsymbol{u}^k_b + F_2 \boldsymbol{u}^k_2 \qquad k = 1, 2, \ldots, N_l$$

$$\boldsymbol{\sigma}^k_{nM} = F_t \boldsymbol{\sigma}^k_{nt} + F_b \boldsymbol{\sigma}^k_{nb} + F_2 \boldsymbol{\sigma}^k_{n2} \quad (3)$$

where

$$F_t = \frac{1+\zeta_k}{2}, \qquad F_b = \frac{1-\zeta_k}{2}, \qquad F_2 = \frac{2}{3}\left(\zeta^2_k - 1\right)$$

Received 16 March 1998; revision received 26 January 1999; accepted for publication 5 February 1999.

*Research Professor, Department of Aeronautics and Aerospace Engineering, Corso Duca degli Abruzzi, 24; carrera@polito.it. Member AIAA.

Table 1 List of the acronyms used to denote three-dimensional and two-dimensional plate theories, in alphabetic order

Designation	Description
CLT	Classical lamination theory
D-l$^{N_l^*}$, D-p$^{N_l^*}$	Present LWMs based on displacements formulation, l and p refer to linear and parabolic expansion, N_l^* is the numbers of mathematical interfaces
ESLM	Present equivalent single-layer model
E-l, E-p	Present ESLM with linear and parabolic displacements fields [Eqs. (4) and (5)]
E-la	E-l implementing shear correction factor
E-lb	E-l neglecting transverse normal stress
E-lc	E-lb implementing shear correction factor
Exact	Three-dimensional solutions in Refs. 2 and 3
FSDT	First-order shear deformation theory
F-R	FSDT by Reddy[16]
F-J&T	FSDT taken by Jing and Tzeng[4]
HSDT	Higher-order shear deformation theory
H-B&V	HSDT by Bhaskar and Varadan[5]
H.a-B&V	H-B&V results with shear stress computed by assumed models.
H.b-B&V	H-B&V results with shear stress computed via integration of three-dimensional equilibrium equations
H-D&P	HSDT by Dennis and Palazotto[7]
H-J&T	HSDT by Jing and Tzeng[4]
H-K&al	HSDT by Librescu et al.[15]
H-R&L	HSDT by Reddy and Liu[16]
LWM	Layerwise model
M-p$^{N_l^*}$, M-l$^{N_l^*}$	Present mixed LWMs [Eqs. (2) and (3)]
.Δ	Donnell-type approximations

and $\zeta_k = z_k/(2h_k)$ is a nondimensioned transverse coordinate (h_k denotes the layer thickness). Expansion restricted to the displacement fields is used in the two cases (D-p and D-l) based on displacement formulation. Fictitious, mathematical interfaces have been introduced in the calculation both to improve the displacement and stress fields and to reduce the curvature approximations related to the thickness to radii shell ratio h/R (as in Ref. 1 the geometrical parameters that are not affected by the k superscript or subscript refer to the whole multilayered shell reference surface Ω). The total number of interfaces is denoted by N_l^*. If it is different than N_l, it will be shown as a superscript (or in brackets in the figures) in correspondence to the acronyms of the considered layerwise results. The two following cases are implemented next: $N_l^* = 2 \times N_l$ and $N_l^* = 5 \times N_l$.

B. Equivalent Single-Layer Models

As discussed in Appendix A of Ref. 1, equivalent single-layer theories have been restricted to the displacement formulation. To obtain classical theories as particular cases, the use of power expansion in terms of the whole thickness coordinate z (centered at the shell middle surface) has been preferred to the Legendre polynomials.

First the quadratic expansion has been considered (E-p):

$$\boldsymbol{u} = F_t \boldsymbol{u}_t + F_b \boldsymbol{u}_b + F_2 \boldsymbol{u}_2 \tag{4}$$

where

$$F_t = 1, \qquad F_b = z, \qquad F_2 = z^2$$

and are now given in terms of the multilayered shell coordinate z. The variable $\boldsymbol{u}_t$ takes on the meaning of displacement vector in correspondence to the middle surface Ω of the shell, while $\boldsymbol{u}_b$ and $\boldsymbol{u}_2$ assume the meaning of the first and second variation of $\boldsymbol{u}$ on Ω, respectively.

The linear case (E-l) is written simply as

$$\boldsymbol{u} = F_t \boldsymbol{u}_t + F_b \boldsymbol{u}_b \tag{5}$$

The shear correction factor χ can be associated to the previous model (E-la): the value $\chi = \frac{5}{6}$ is referred to. Transverse normal strain effects can be considered in an easier manner than the Legendre expansion. It is sufficient to discard the linear term in the expansion of the transverse component u_z in Eq. (5). The resulting model (E-lb) is almost coincident with the well-known first-order shear deformation theory (FSDT). E-lc corresponds to the case in which a shear correction factor is introduced into the E-lb analysis.

III. Results and Discussion

In this section implemented theories are compared to the exact analyses given by Refs. 2 and 3 and to other ESLM analyses that are known as higher-order shear deformation theories (HSDT) (Table 1). The two HSDT models by Jing and Tzeng[4] and Bhaskar and Varadan,[5] where the Reissner mixed variational equation was employed to derive ESLM theories, are of particular interest.

In-plane and out-of-plane displacement and stress components are compared. The values of the transverse shear and normal stresses related to the present investigation are those a priori calculated directly by the assumed stress model in Eqs. (2) and (3), i.e., they are available only for the mixed cases. Displacement formulations would require the use of a postprocessing procedure, e.g., integration of the indefinite equilibrium equations. This postprocessing procedure has not been implemented at this stage. In this respect, the results that have already been obtained for plates should be expected.[6] Values corresponding to the plate point in which the stresses and displacements assume their maximum amplitudes in Eqs. (1) are shown in the figures, which give the distribution of these amplitudes (as ordinate) vs the plate thickness direction (as abscissa). In all of the considered analyses the shells are bent by a transverse harmonic distribution of normal pressure applied to the top (external) or bottom (internal) surface of the whole shell. Symmetrically and unsymmetrically laminated, as well as sandwich thick and thin shells, have been analyzed. A vast numerical investigation has been conducted. The most significant results are described in the following sections.

A. Ren's Cylindrical Panels

Exact solutions were considered by Ren[2] for cylindrical panels cross-ply laminated in cylindrical bending. The case of a transverse pressure applied to the top (external) layer was considered:

$$p_{z_t}^{N_l} = \sum_n P_{z_t}^{N_l} \sin \frac{n\pi\beta}{b} \tag{6}$$

The geometrical data (Fig. 1) are $n = 1$, $R_\beta/b = \pi/3$, and the mechanical data are $E_L = 25 \times 10^6$ psi (172 GPa), $E_T = 10^6$ psi (6.9 GPa), $G_{LT} = 0.5 \times 10^6$ psi (3.4 GPa), $G_{TT} = 0.2 \times 10^6$ psi (1.4 GPa), $\nu_{LT} = \nu_{TT} = 0.25$, where, following the usual notations, L signifies the fiber direction, T the transverse direction, and ν_{LT} is the major Poisson ratio. The material is assumed to be square-symmetric and consistent units are referred to. Laminas of equal thickness are analyzed. Four cross-plied panels are considered according to the following lamination schemes: one layer, 90 deg; two layers, 0/90 deg; three layers, 90/0/90 deg; five layers, 90/0/90/0/90 deg. Layers are numbered, starting from the shell bottom (internal surface). It is also intended that the fiber L orientation coincides with the α_k-layer directions.

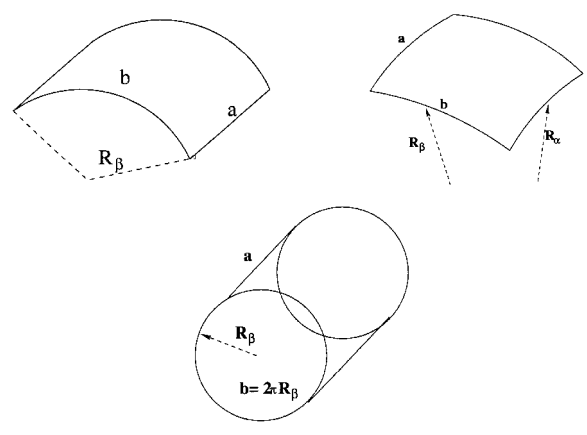

Fig. 1 Geometrical notations used for the investigated cylindrical panels, spherical panels, and cylindrical shells.

Table 2 Comparison of present analyses to three-dimensional exact solutions by Ren[2] (case a: single-layer case, 90 deg; transverse displacement and transverse shear stress amplitude)

R_β/h	2	4	10	50	100
		$\bar{U}_z = U_z \times (10E_T h^3/P^1_{z_b} R^4_\beta),\ z=0$			
Exact	0.9986	0.312	0.115	0.077	0.0755
CLT	0.0764	0.0752	0.0749	0.0748	0.0748
H-D&P	0.803	0.278	0.108	0.0762	0.0751
		Present LWM			
M-p	1.094	0.3219	0.1151	0.0770	0.0755
M-p^2	1.030	0.3140	0.1147	0.0770	0.0755
M-p^5	1.000	0.3121	0.1146	0.0770	0.0755
M-p^5.Δ	0.7790	0.2450	0.0905	0.0608	0.0597
M-l^2	1.183	0.3466	0.1190	0.0771	0.0756
M-l^5	0.9727	0.3097	0.1156	0.0770	0.0755
D-p	0.8905	0.2778	0.1087	0.0767	0.0755
D-p^2	0.9628	0.3071	0.1142	0.0770	0.0755
D-p^5	0.9940	0.3117	0.1146	0.0770	0.0755
D-l	0.9104	0.2793	0.1085	0.0764	0.0752
D-l^2	0.8787	0.2773	0.1087	0.0767	0.0754
D-l^5	0.9606	0.3040	0.1134	0.0770	0.0755
		Present ESLM			
E-p	0.9704	0.2874	0.1090	0.0767	0.0754
E-l	0.8933	0.2781	0.1085	0.0764	0.0752
E-l.Δ	0.6980	0.2181	0.0854	0.0602	0.0593
E-la	1.054	0.3171	0.1146	0.0767	0.0752
E-lb	0.9784	0.2798	0.1076	0.0764	0.0752
E-lc	1.123	0.3191	0.1135	0.0766	0.0752
		$\bar{S}_{\beta z} = \lvert S_{\beta z} \times (h/P^1_{z_b} R_\beta)\rvert,\ z=0$			
Exact	0.555	0.572	0.579	0.568	0.565
M-p	0.7031	0.6328	0.5906	0.5681	0.5653
M-p^2	0.4614	0.5295	0.5699	0.5673	0.5661
M-p^5	0.5673	0.5715	0.5796	0.5677	0.5652

Table 3 Comparison of present analyses to three-dimensional exact solutions by Ren[2] [case b: antisymmetric two-layer case, 0/90 deg; transverse displacement amplitude; $\bar{U}_z = U_z \times (10E_T h^3/P^1_{z_b} R^4_\beta)$ at $z = 0$]

R_β/h	2	4	10	50	100
Exact	2.079	0.854	0.493	0.409	0.403
CLT	0.499	0.447	0.417	0.402	0.400
		Present LWM			
M-p	2.111	0.8570	0.4935	0.4088	0.4032
M-p^4	2.087	0.8543	0.4932	0.4088	0.4032
M-p^{10}	2.080	0.8537	0.4932	0.4088	0.4032
M-p^{10}.Δ	1.571	0.6539	0.3841	0.3221	0.3181
M-l	2.005	0.8477	0.4985	0.4089	0.4033
M-l^4	2.046	0.8541	0.4938	0.4088	0.4032
M-l^{10}	2.082	0.8539	0.4932	0.4088	0.4032
D-p	1.968	0.8232	0.4880	0.4086	0.4031
D-p^4	2.070	0.8513	0.4928	0.4088	0.4031
D-p^{10}	2.078	0.8535	0.4932	0.4088	0.4031
D-l	1.894	0.8081	0.5945	0.4066	0.4012
D-l^4	1.950	0.8195	0.4871	0.4081	0.4026
D-l^{10}	2.052	0.8470	0.4920	0.4087	0.4031
		Present ESLM			
E-p	2.007	0.8100	0.4839	0.4080	0.4028
E-l	1.849	0.7815	0.4737	0.4014	0.3964
E-l.Δ	1.383	0.5893	0.3635	0.3135	0.3103
E-la	2.096	0.8725	0.4942	0.4023	0.3972
E-lb	1.914	0.7847	0.4730	0.3986	0.3984
E-lc	2.174	0.8425	0.4815	0.3990	0.3935

Tables 2–4 compare the present analyses to exact solutions and to the previously mentioned HSDT results. In particular, the theory H-D&P[7] fulfills the homogeneous conditions for the transverse shear stresses. Interlaminar equilibrium is also fulfilled by the H-B&V[5] analysis. One-, two-, and three-layered panels are considered in Tables 2, 3, and 4, respectively. Transverse displacement and transverse shear stress values are compared. The first four digits are usually shown. CLT solutions are also taken from Ref. 2. Five different thickness ratios have been investigated. The layerwise analysis implements fictitious interfaces. For the one-layer case the mixed solution has been restricted to the parabolic expansion. In the case of a multilayered shell, top-bottom homogeneous conditions for the transverse shear stress could not be imposed for the linear expansion of Eqs. (2). In fact, their linkage would require discarding the stiffness and/or compliance contributions related to the top and bottom shell layers. These conditions have therefore not been considered in all the illustrated M-l results. The following comments can be made about the Table 2–4 results:

Table 4 Comparison of present analyses to three-dimensional exact solutions by Ren[2] (case c: symmetric three-layer case, 90/0/90 deg; transverse displacement and transverse shear stress amplitude)

R_β/h	2	4	10	50	100
		$\bar{U}_z = U_z \times (10E_T h^3/P^1_{z_b} R^4_\beta),\ z=0$			
Exact	1.436	0.457	0.144	0.0808	0.0787
CLT	0.0799	0.0781	0.0777	0.0776	0.0776
H-D&P	1.141	0.382	0.128	0.0796	0.0781
H-J&T	——	0.459	0.142	0.0802	0.0780
F-J&T	——	0.342	0.120	0.0793	0.0780
		Present LWM			
M-p	1.456	0.4593	0.1440	0.0808	0.0786
M-p^6	1.438	0.4582	0.1440	0.0808	0.0786
M-p^{15}	1.436	0.4582	0.1440	0.0808	0.0787
M-l	1.369	0.4424	0.1425	0.0808	0.0786
M-l^6	1.409	0.4564	0.1440	0.0808	0.0786
M-l^6	1.434	0.4581	0.1440	0.0808	0.0787
D-p	1.398	0.4543	0.1440	0.0808	0.0786
D-p^6	1.431	0.4579	0.1440	0.0808	0.0786
D-p^{15}	1.436	0.4582	0.1440	0.0808	0.0786
D-l	1.363	0.4407	0.1439	0.0807	0.0785
D-l^6	1.378	0.4506	0.1431	0.0808	0.0786
D-l^{15}	1.424	0.4568	0.1439	0.0808	0.0786
		Present ESLM			
E-p	1.183	0.3391	0.1192	0.0779	0.0783
E-l	1.108	0.3300	0.1187	0.0795	0.0780
E-l.Δ	0.8682	0.2591	0.0935	0.0627	0.0615
E-la	1.311	0.3787	0.1263	0.0798	0.0781
E-lb	1.164	0.3317	0.1179	0.0794	0.0780
E-lc	1.379	0.3808	0.1253	0.0797	0.0780
		$\bar{S}_{\beta z} = \lvert S_{\beta z} \times (h/P^1_{z_b} R_\beta)\rvert,\ z=0$			
Exact	0.394	0.476	0.525	0.526	0.523
H-D&P	0.287	0.326	0.340	0.334	0.217
H-J&T	——	0.511	0.574	0.576	0.574
F-J&T	——	0.225	0.225	0.225	0.225
M-p	0.402	0.487	0.527	0.525	0.523
M-p^{15}	0.391	0.476	0.525	0.526	0.523

1) Excellent agreement between M-p and exact results has been found for both displacement and transverse stresses even though very thick panels were considered. A better description with respect to the related layerwise analyses based on displacement formulations should be registered.

2) An acceptable convergence rate of the layerwise model has been found for thick shells. Because of the further approximations concerning curvature terms, such a rate is slower than those found for the plate cases[8] (see also the discussion by Jing and Tzeng[4] and Voyiadis and Shi[9]).

3) For the one-layer case M-p, D-p, and D-l consist of ESLM results. Approximations related to curvature effects are more evident in this case.

4) D-l analysis can lead to a better description of the deflections with respect to the D-p cases. This unexpected result must be considered because a local value is concerned (see discussion of Table 5–7 results).

5) The accuracy of the LW results is independent of the lamination scheme. As verified for the plate cases,[6] the already mentioned HSDT analyses (D&P, J&T) give a better accuracy in the case of symmetric through the thickness distribution of displacement and stress fields. In fact, the results were restricted to symmetrically laminated panels in these papers. It has also been confirmed that the use of shear correction factors, being problem dependent,[10,11] could be meaningless for thick shell analyses.

6) Results related to different theories merge for thin shells.

7) As Donnell's approximationsare related to the R_β/b ratio these are not affected by the R_β/h ratio.

It is of certain interest to notice that stress and displacement formulations lead to a lower and higher estimate of the shell stiffness as far as the exact three-dimensional solutions are concerned. In fact, D-p and D-l displacement values are always lower than the exact ones. In the mixed cases a unique conclusion cannot be drawn: This very much depends on the relative role played by the in-plane and out-of-plane energy and the results obviously become problem dependent. For most of the considered problems it has been found that mixed and displacement solutions lead to higher and lower approximations for the displacements, respectively.

The thickness distributions of displacement and transverse stress amplitudes have been plotted in Figs. 2–6. Figure 2 compares present mixed and displacements layerwise studies to Ren's exact results,[2] and FSDT and HSDT solutions by Jing and Tzeng.[4] For the exact case, only interface values have been drawn. When different from N_l the mathematical interfaces used have been indicated in brackets. The excellent agreement of the proposed mixed analysis in comparison with the exact ones found in Tables 2–4 has been confirmed. The superiority of the mixed analysis with respect to the displacement one becomes more evident for lower N_l^* values. A fundamental limitation of the ESLM analysis also emerges: Even though ESLMs are based on mixed principles, as is the case of Ref. 4, they cannot improve the shell response in whole thickness fields[6,12] transverse normal stress and related effects are neglected in Ref. 4. An excellent agreement with the exact solution has been confirmed for the transverse shear stress case of Fig. 3. Larger errors have to register by the stress evaluated in Ref. 4 with respect to the M-p results (stresses related to the J&T results are those obtained via integration of the

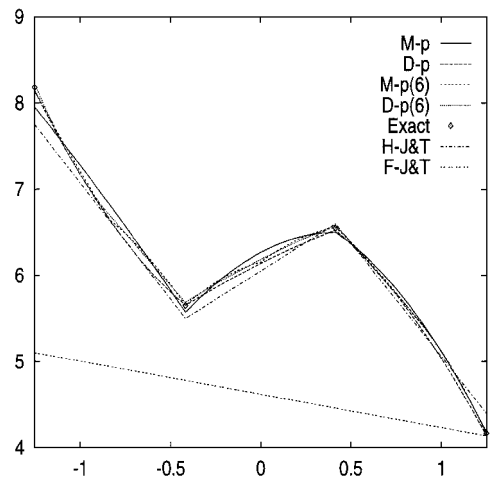

Fig. 2 Amplitude of in-plane displacement $\bar{U}_\beta = U_\beta \times (100E_T h^2/P_{z_t}^{N_l} R_\beta^3)$ vs z: Ren's cylindrical panel with $R_\beta/h = 4$; three-layer case.

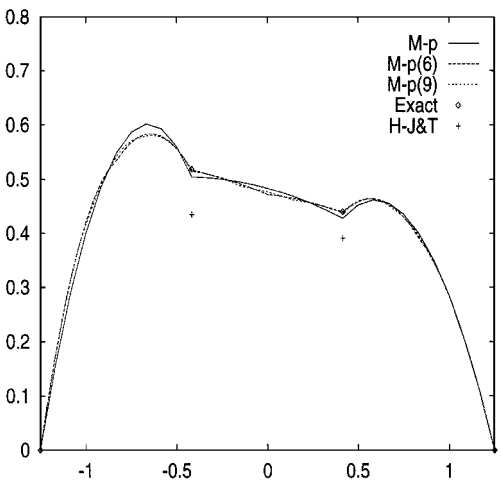

Fig. 3 Amplitude of transverse shear stress $\bar{S}_{\beta z} = |S_{\beta z} \times (h/P_{z_t}^{N_l} R_\beta)|$ vs z: Ren's cylindrical panel with $R_\beta/h = 4$; three-layer case.

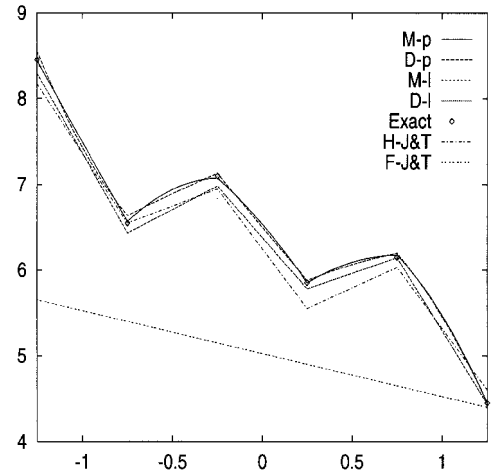

Fig. 4 Amplitude of in-plane displacements $\bar{U}_\beta = U_\beta \times (100E_T h^2/P_{z_t}^{N_l} R_\beta^3)$ vs z: Ren's cylindrical panel with $R_\beta/h = 4$, five-layer case.

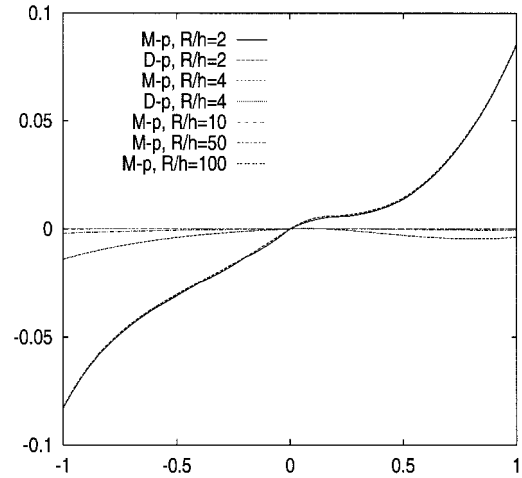

Fig. 5 Effect of R_β/h on the amplitude of the transverse displacement increment $\bar{U}_z - \bar{U}_c = (U_z - U_c) \times (10E_T h^3/P_{z_t}^{N_l} R_\beta^4)$ vs $z/2h$: two-layer case of Ren's cylindrical panel.

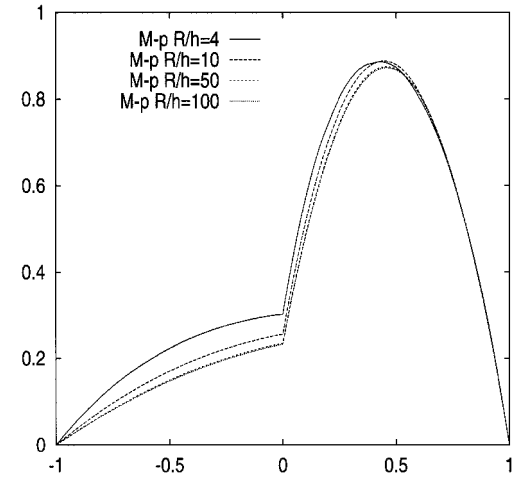

Fig. 6 Effect of R_β/h on the amplitude of transverse shear stress $\bar{S}_{\beta z} = S_{\beta z} \times (h^2/-P_{z_b}^1 R_\beta^2)$ vs $z/2h$: Ren's cylindrical panel; two-layer case.

three-dimensional elasticity indefinite equilibrium equations). The preceding comments have been confirmed for the five-layer case illustrated in Fig. 4. The linear case of layerwise results are also considered in this plot. Only physical interfaces have been used in this diagram. Several thickness ratios are considered in Fig. 5 for the two-layer case. The D-p results are only shown for thicker shells. The increments from their values measured at $z = 0$ (given in Table 2 and denoted by U_c) are considered. Ten mathematical

interfaces have been used in the calculation to guarantee convergent solutions. Because of the transverse strain effects, it has been shown that thicker plates manifest higher variations of transverse displacement as well as nonsymmetric distributions. The same laminate is considered in Fig. 6, where transverse shear stress is evaluated (see also the exact solution in Ref. 2). It should be noticed that, even for thin shells, the parabolic distribution of shear stresses, usually assumed by corrected FSDT analysis, could become meaningless for these asymmetrically laminated panels.

B. Varadan and Bhaskar's Cylindrical Shells

Varadan and Bhaskar[3] considered exact solutions for cross-ply laminated, cylindrical shells, subjected to transverse pressure at the bottom (internal) surface,

$$p^1_{z_b} = \sum_{m,n} P^1_{z_b} \sin\frac{m\pi\alpha}{a} \sin\frac{n\pi\beta}{b} \tag{7}$$

The geometrical data are (see Fig. 1): $a/R_\beta = 4$, $m = 1$, $n = 8$. The mechanical data are $E_L/E_T = 25$, $G_{LT}/E_T = 0.5$, $G_{TT}/E_T = 0.2$, $\nu_{LT} = \nu_{TT} = 0.25$. The following lamination schemes have been considered: 2 layers, 0/90 deg; 3 layers, 90/0/90 deg; 4 layers, 90/0/90/0 deg; 5 layers, 90/0/90/0/90 deg; and 10 layers, $[90/0/90/0/90\ \text{deg}]_s$.

Wherever available, comparisons are made with other HSDT solutions that were given by the same authors[5] by using a Reissner mixed variational equation to derive ESLM studies. A less accurate description of curvature terms in comparison to that in Ref. 4 is furnished by the results in Ref. 5. Results on transverse normal stresses are quoted in Tables 5–7 in addition to what has been done

Table 5 Comparison of present analyses to three-dimensional exact solutions by Varadan and Bhaskar[3] for cylindrical shells (case a: antisymmetric two-layer case, 0/90 deg; transverse displacement, transverse shear, and normal stress amplitudes)

R_β/h	2	4	10	50	100
		$\tilde{U}_z = U_z \times (10E_L h^3/P^1_{z_b} R^4_\beta), z = 0$			
Exact	14.034	6.100	3.330	2.242	1.367
		Present LWM			
M-p	14.309	6.107	3.352	2.242	1.367
M^4-p	14.098	6.100	3.330	2.242	1.367
M^{10}-p	14.040	6.100	3.330	2.242	1.367
M-p^{10} (t)	11.659	5.797	3.311	2.241	1.367
M-p^{10} (b)	19.458	6.378	3.318	2.242	1.367
M-p^{10}.Δ	12.156	5.254	2.015	2.015	1.279
M-l	13.012	5.999	3.329	2.243	1.368
M-l^4	13.622	6.068	3.334	2.242	1.367
M-l^{10}	14.054	6.102	3.330	2.242	1.367
D-p	13.397	5.848	3.275	2.241	1.367
D-p^4	13.949	6.078	3.326	2.242	1.367
D-p^{10}	14.021	6.099	3.330	2.242	1.367
D-l	12.539	5.688	3.246	2.231	1.364
D-l (t)	10.176	5.379	3.227	2.231	1.364
D-l (b)	17.395	5.948	3.235	2.231	1.364
D-l^4	13.182	5.808	3.268	2.238	1.365
D-l^{10}	13.851	6.042	3.332	2.242	1.367
E-p	13.213	5.830	3.310	2.247	1.369
		Present ESLM			
E-l	13.041	5.567	3.171	2.208	1.356
E-l (t)	9.798	5.188	3.167	2.208	1.356
E-l (b)	16.625	5.755	3.175	2.208	1.356
E-l.Δ	11.233	4.748	2.726	1.975	1.265
E-la	15.133	6.141	3.265	2.212	1.356
E-lb	12.155	5.463	3.172	2.205	1.356
E-lc	14.062	6.016	3.266	2.207	1.356
		$\bar{S}_{z\beta} = S_{z\beta} \times (10h/P^1_{z_b} R_\beta), z = -1/4$			
Exact	−2.931	−4.440	−5.457	−4.785	−2.972
M-p^4	−2.716	−4.316	−5.427	−4.783	−2.972
M-p^{10}	−2.951	−4.450	−5.459	−4.785	−2.972
		$\bar{S}_{zz} = S_{zz} \times (1/P^1_{z_b}), z = 1/4$			
Exact	−0.31	−0.70	−1.68	−6.29	−7.71
M^4-p	−0.30	−0.69	−1.68	−6.21	−7.70
M^{10}-p	−0.32	−0.70	−1.67	−6.29	−7.70

Table 6 Comparison of present analyses to three-dimensional exact solutions by Varadan and Bhaskar[3] for cylindrical shells (case b: symmetric three-layer case, 90/0/90 deg)

R_β/h	2	4	10	50	100
		$\tilde{U}_z = U_z \times (10E_L h^3/P^1_{z_b} R^4_\beta), z = 0$			
Exact	10.11	4.009	1.223	0.5495	0.4715
H-B&V	——	3.923	1.210	——	——
		Present LWM			
M-p	10.335	4.007	1.223	0.5495	0.4715
M-p^6	10.149	4.009	1.223	0.5495	0.4715
M-p^{15}	10.114	4.009	1.223	0.5495	0.4715
M-p^{15}.Δ	8.862	3.532	1.077	0.4857	0.4222
D-p	9.638	3.949	1.221	0.5495	0.4715
D-p^6	10.005	4.004	1.223	0.5495	0.4715
D-p^{15}	10.109	4.007	1.223	0.5495	0.4715
D-p^{15}.Δ	8.856	3.536	1.077	0.4857	0.4222
		Present ESLM			
E-p	8.954	2.917	0.944	0.5384	0.4694
E-l	8.739	2.998	0.953	0.5358	0.4674
E-l.Δ	7.679	2.638	0.837	0.4729	0.4180
E-la	10.397	3.495	1.040	0.5392	0.4682
E-lb	8.393	2.864	0.935	0.5418	0.4666
E-lc	9.979	3.340	1.018	0.5380	0.4673
		$\bar{S}_{z\beta} = S_{z\beta} \times (10h/P^1_{z_b} R_\beta), z = 0$			
Exact	−1.379	−2.349	−3.264	−3.491	−3.127
M-p	−1.421	−2.399	−3.283	−3.492	−3.127
M-p^6	−1.374	−2.352	−3.253	−3.492	−3.127
M-p^5	−1.380	−2.349	−3.253	−3.491	−3.127
		$\bar{S}_{zz} = S_{zz} \times (1/P^1_{z_b}), z = 0$			
Exact	−0.34	−0.62	−1.27	−4.85	−8.30
M-p	−0.33	−0.60	−1.24	−4.73	−8.29
M-p^6	−0.34	−0.62	−1.25	−4.85	−8.30
M-p^{15}	−0.34	−0.62	−1.27	−4.85	−8.30

Table 7 Comparison of present analyses to three-dimensional exact solutions by Varadan and Bhaskar[3] for cylindrical shells (case c: symmetric ten-layer case, $[90/0/90/0/90\ \text{deg}]_s$)

R_β/h	2	4	10	50	100
		$\tilde{U}_z = U_z \times (10E_L h^3/P^1_{z_b} R^4_\beta), z = 0$			
Exact	11.44	4.206	1.380	0.7622	0.6261
H-B&V	——	4.064	1.353	——	——
		Present LWM			
M-p	11.441	4.206	1.380	0.7622	0.6261
M-p^{20}	11.439	4.206	1.380	0.7622	0.6261
M-l	11.370	4.194	1.379	0.7622	0.6261
M-l^{20}	11.419	4.205	1.380	0.7622	0.6261
D-p	11.412	4.205	1.380	0.7622	0.6261
D-p^{20}	11.435	4.205	1.380	0.7622	0.6261
D-l	11.282	4.175	1.375	0.7620	0.6261
D-l^{20}	11.379	4.198	1.378	0.7622	0.6261
		Present ESLM			
E-p	9.395	3.240	1.200	0.7564	0.6252
E-l	9.360	3.323	1.205	0.7517	0.6221
E-la	11.105	3.748	1.296	0.7552	0.6299
E-lb	8.965	3.192	1.187	0.7505	0.6211
E-lc	10.648	3.689	1.274	0.7537	0.6216
		$\bar{S}_{z\beta} = S_{z\beta} \times (10h/P^1_{z_b} R_\beta), z = 0$			
Exact	−2.608	−3.154	−3.479	−3.425	−2.884
M-p	−2.581	−3.137	−3.475	−3.425	−2.884
M-p^{20}	−2.601	−3.150	−3.478	−3.425	−2.884
M-l	−2.863	−3.235	−3.426	−3.342	−2.884
M-l^{20}	−2.648	−3.183	−3.497	−3.440	−2.884
		$\bar{S}_{zz} = S_{zz} \times (1/P^1_{z_b}), z = 0$			
Exact	−0.42	−0.71	−1.32	−4.76	−7.69
M-p	−0.42	−0.71	−1.32	−4.76	−7.69
M-p^{20}	−0.42	−0.71	−1.32	−4.76	−7.69
M-l	−0.42	−0.70	−1.32	−4.76	−7.69
M-l^{20}	−0.42	−0.71	−1.32	−4.76	−7.79

for Ren's cylindrical panels. The conclusions and comments reached for the cylindrical panels can be extended to cylindrical shells. The accuracy found for the transverse shear stress has to be confirmed for the transverse normal stress. Table 5 investigated the two-layers case. As for cylindrical panels, transverse displacements computed at $z = 0$ related to D-l seems to be more accurate than D-p. However, this is just a local phenomena as can be demonstrated by comparing the related top t and bottom b shell surface values to those corresponding to the M-p analysis. The same comments can be made for the E-l analysis. The effects of shear correction factor remains unforeseeable for thick shell results. Three- and ten-layer cases are considered in Tables 6 and 7. Increasing accuracy is obtained by layerwise analyses for higher number of the N_l layers. Naturally, a better description of the curvatures terms is obtained in these cases. This is not the case of ESLM studies. Nevertheless, H-B&V results very much improve classical ESLM analysis.

The distributions of stress and displacements have been plotted in the subsequent Figs. 7–10. Figure 7 compares layerwise results related to transverse displacement distributions for a three-layer case. Case $N_l^* = 6$ has also been considered. Larger through-the-thickness variation of u_z should be registered for the thick shell considered. A comparison to exact and HSDT results by Bhaskar and Varadan[3] are provided in the remaining figures. Transverse shear stress for a three- and five-layer case is considered in Figs. 8 and 9. An excellent agreement between the exact studies and the present M-p evaluations can be seen. A poor description was found for the ESLM analysis in Ref. 5 even though the transverse shear stresses were evaluated

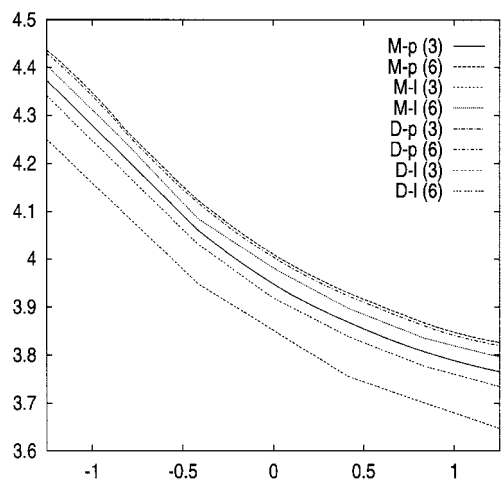

Fig. 7 Amplitude of transverse displacement $\bar{U}_z = U_z \times (10E_L h^3/P^1_{z_b} R^4_\beta)$ vs z: comparison of present LW results; Varadan and Bhaskar's cylindrical shells with $R_\beta/h = 4$; three-layer case.

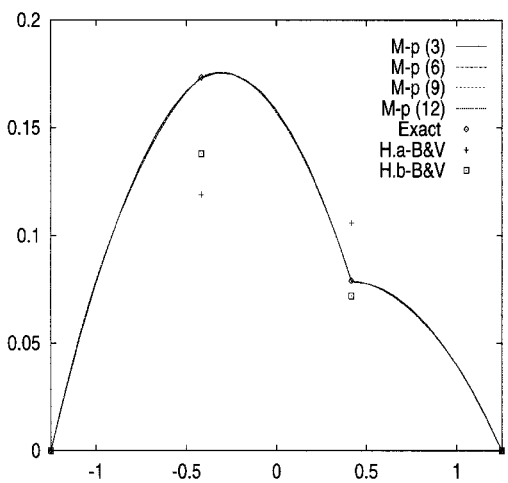

Fig. 8 Amplitude of transverse shear stress $\bar{S}_{\alpha z} = S_{\alpha z} \times (10h/P^1_{z_b} R_\beta)$ vs z: Varadan and Bhaskar's cylindrical shells with $R_\beta/h = 4$; three-layer case.

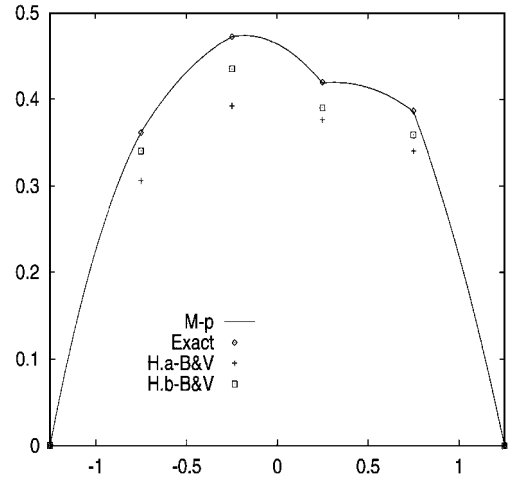

Fig. 9 Amplitude of transverse shear stress $\bar{S}_{\alpha z} = |S_{\alpha z} \times (10h/P^1_{z_b} R_\beta)|$ vs z: Varadan and Bhaskar's cylindrical shells with $R_\beta/h = 4$; five-layer case.

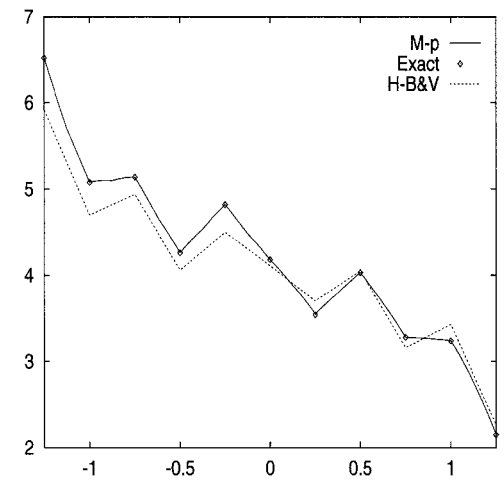

Fig. 10 Amplitude of in-planer displacements $\bar{U}_\beta = U_\beta \times (10E_L h^2/P^1_{z_b} R^3_\beta)$ vs z: Varadan and Bhaskar's cylindrical shells with $R_\beta/h = 4$; 10-layer case.

via integration of the three-dimensional indefinite equilibrium equations (H.b-B&V). One should notice that the evaluations given in Ref. 5 are not always conservative. Furthermore, the related transverse shear stresses evaluated a priori (H.a-B&V) demonstrate, as it was found for plates,[13,14] that such an evaluation requires a layerwise description. A ten-layer case is considered in Fig. 10 where the distribution of the in-plane displacement has been plotted. One could conclude that as N_l increases the accuracy of the ESLM result decreases whereas that of LWM increases.

C. Solution for Spherical Shells

Only a few results for the spherical shell, square panels have been considered in this section. These panels are loaded by a harmonic distribution of pressure applied in correspondence to the external surface:

$$p^1_{z_b} = \sum_{m,n} P^{N_l}_{z_t} \sin\frac{m\pi\alpha}{a} \sin\frac{n\pi\beta}{b} \tag{8}$$

The geometrical data (see Fig. 1) are $a/h = 5$, $a/b = 1$, $m = 1$, $n = 1$. The mechanical data are $E_L/E_T = 25$, $G_{LT}/E_T = 0.5$, $G_{TT}/E_T = 0.2$, $\nu_{LT} = \nu_{TT} = 0.25$, $\nu_{TT} = 0.49$.

Tables 8 and 9 give a comparison of the present studies with the ESLM ones by Librescu et al.[15] and Reddy and Liu,[16] for two- and three-layer cross-plied cases, respectively. Increasing $R = R_\alpha = R_\beta$ values are considered. Quite different results were found from the referenced ESLM analyses, most of which were given under

Table 8 Present analysis vs other ESLMs results: spherical panel [case a: two-layer case, 90/0 deg; transverse displacement amplitude $\bar{U}_z = U_z \times (10^3 E_T h^3 / P_{z_t}^{N_l} a^4), z = 0$]

R/a	1	2	5	10	100
F-R	4.023	8.156	11.43	12.16	12.37
H-R&L	——	——	11.17	11.90	12.16
H-K&al	——	——	11.29	11.20	12.26
H-K&al	——	——	12.01	11.91	12.17
		Present ESLM			
E-p	4.357	8.336	11.25	11.80	11.92
E-l	4.299	7.977	10.52	10.99	11.09
E-l.Δ	4.022	7.715	10.45	10.96	11.09
E-la	4.330	8.119	10.78	11.27	11.38
E-lb	4.284	7.969	10.53	10.99	11.09
E-lc	4.320	8.107	10.78	11.27	11.38
		Present LWM			
M-p	4.184	8.181	11.34	12.01	12.25
M-p.Δ	3.889	7.912	11.25	11.99	12.25
M-p[6]	4.148	8.180	11.34	12.01	12.25
M-l	4.133	8.159	11.31	11.99	12.23
M-l.Δ	3.871	7.887	11.22	11.96	12.23
M-l[6]	4.149	8.182	11.34	12.01	12.25
D-p	4.131	8.120	11.23	11.89	12.12
D-p.Δ	3.871	7.853	11.14	11.86	12.12
D-p[6]	4.148	8.179	11.34	12.01	12.25
D-l	4.099	8.002	11.01	11.63	11.86
D-l.Δ	3.873	7.735	10.92	11.61	11.86
D-l[6]	4.138	8.138	11.26	11.92	11.25

Table 9 Present analysis vs other ESLMs results: spherical panel (case b: three-layer case, 90/0/90 deg)

R/a	1	2	5	10	100
F-R	3.259	5.305	6.425	6.625	6.692
H-R&L	——	——	6.769	7.033	7.124
H-K&al	——	——	6.625	6.862	6.944
H-K&al	——	——	6.625	6.806	6.886
		Present ESLM			
E-p	3.495	5.281	6.119	6.231	6.235
E-l	3.464	5.195	5.997	6.105	6.110
E-l.Δ	3.164	5.001	5.953	6.093	6.110
E-la	3.551	5.439	6.349	6.476	6.486
E-lb	3.454	5.192	6.002	6.109	6.110
E-lc	3.541	5.453	6.355	6.481	6.487
		Present LWM			
M-p	3.348	5.756	7.129	7.401	7.513
M-p.Δ	3.196	5.548	7.076	7.398	7.513
M-p[9]	3.479	5.574	7.128	7.401	7.513
M-l	3.466	5.728	7.094	7.366	7.478
M-l.Δ	3.182	5.521	7.042	7.531	7.477
M-l[9]	3.478	5.574	7.128	7.400	7.512
D-p	3.477	5.750	7.121	7.392	7.504
D-p.Δ	3.193	5.546	7.068	7.378	7.503
D-p[9]	3.479	5.754	7.128	7.401	7.513
D-l	3.442	5.652	6.972	7.233	7.341
D-l.Δ	3.157	5.456	6.921	7.220	7.391
D-l[9]	3.474	5.741	7/108	7.378	7.490

Donnell's shallow-shell assumptions. The R/a increasing better results are furnished by Donnell descriptions. To confirm the importance of the curvature terms in LW analysis one should observe the lower discrepancy of the layerwise results related to the different N_l^* when R/a (i.e., R/h) increases.

A few additional studies have been made on the remaining figures. The effect of the orthotropic ratio Re for a four-layered cross-ply spherical panel is considered in Fig. 11. The increasing role played by the zig-zag effects because of increasing anisotropy is displayed. For the $Re = 40$ case, the difference between the M-p and D-p results is barely evident. The transverse shear stress distribution of the same problem has been plotted in Fig. 12. M-p values are given; quite different results are found for different orthotropic ratios. The well-known parabolic distribution is confirmed for lower Re values. A sandwich construction has been considered in Fig. 13 as the last problem. A three-layered cross-ply panel (90/0/90 deg) is considered. The face and core thickness are $h_f = 0.1h$ and $h_c = 0.8h$, respectively. Three different Rf face/core stiffness ratio have been investigated. Because of curvature and the normal stress effects, the displacement fields are not symmetric. As Rf increases the displacement field becomes constant inside the core and the differences between the M-p and D-p results become more evident.

As a drawback the layerwise description requires the use of unknown variables, the number of which depends on the number of

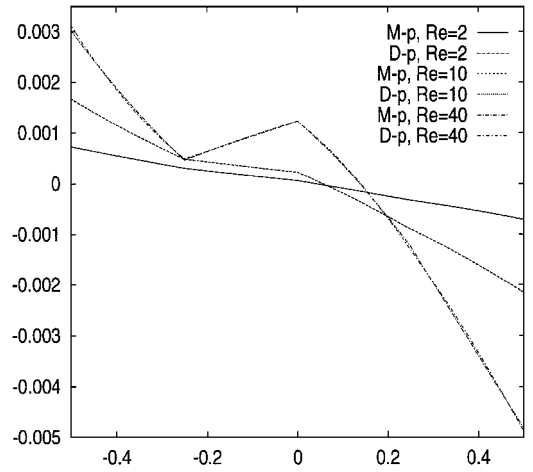

Fig. 11 Effect of orthotropic ratio $Re = E_L/E_t$ on the amplitude of in-plane displacements $\bar{U}_\alpha = U_\alpha \times (10 E_L h^2 / P_{z_t}^{N_l} R^3)$ vs z: spherical shell with $a/h = 5$, $R/h = 50$; four-layer case.

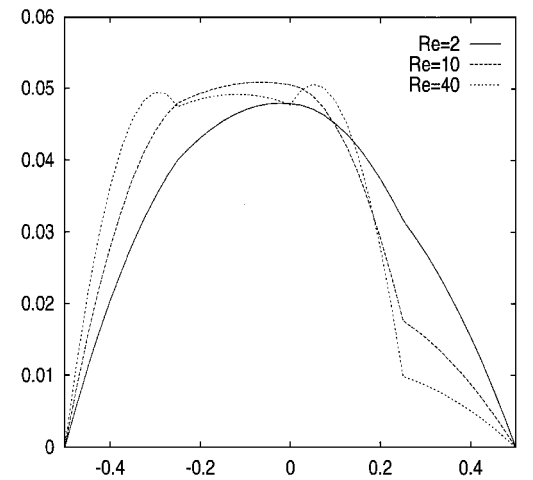

Fig. 12 Effect of orthotropic ratio $Re = E_L/E_t$ on the amplitude of transverse shear stress $\bar{S}_{\alpha z} = S_{\alpha z} \times (h/P_{z_t}^{N_l} R)$ vs z: spherical shell with $a/h = 5$, $R/h = 50$; four-layer case.

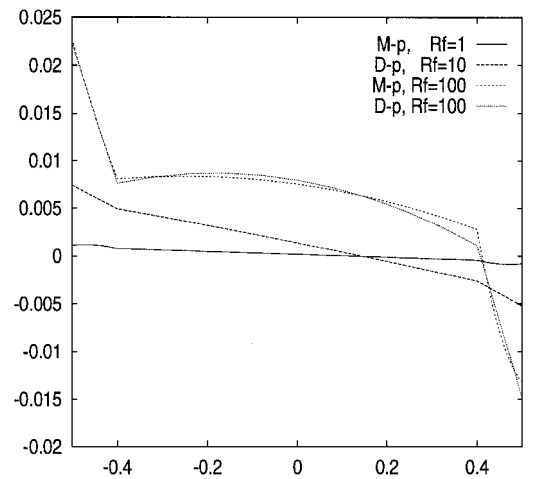

Fig. 13 Effect of face/core stiffness ratio $Rf = (E_L^f/E_L^c)$ on the amplitude of in-plane displacements $\bar{U}_\alpha = U_\alpha \times (100 E_T^f h^2 / P_{z_t}^{N_l} R^3)$ vs z: spherical sandwich shell panel with $a/h = 5$, $R/h = 50$.

layers. Mixed analyses double with respect to models based on displacement formulation. Such a drawback should be taken into account wherever computational models, e.g., finite element applications, have to be developed. Nevertheless, the most expensive layerwise analysis performed in this paper (which is based on simply closed-form solution procedures) took only a few CPU seconds on a standard personal computer. A discussion on the simplified theories on these topics can be read in Ref. 17, where a weak form of Hooke's law was introduced to formulate mixed models as equivalent single-layer models. However, it is the author's opinion that mixed layerwise analysis are required wherever accurate a priori descriptions of transverse stress field are required. Furthermore, the proposed theories preserve the advantages of two-dimensional modeling and lead to an excellent agreement with exact three-dimensional results. This fact should encourage the use of the proposed theories to design multilayered structures or their use to provide reference solutions to assess simplified models.

IV. Conclusions

This paper has evaluated the mixed-layer models that were proposed in the companion paper. The shell equations have been solved for the particular cases of orthotropic lamina cross-ply laminated shells, loaded by a harmonic distribution of transverse pressure. Theories based on displacement formulations have been implemented for comparison purposes. Both layerwise and equivalent single-layer models have been considered. Symmetrically and unsymmetrically as well as sandwich shells have been investigated. Three shell geometries have been investigated: 1) circular cylindrical panels in cylindrical bending for which exact solution were given by Ren,[2] 2) circular cylindrical shells for which exact solutions were given by Varadan and Bhaskar,[3] and 3) spherical square panels.

From the conducted numerical investigations the following main conclusions emerge:

1) The fulfillment of the transverse shear and normal stress interlaminar equilibria has led to a better description as far as the related theory based on displacement formulations is concerned. Excellent agreement has been found for both local and global values with respect to exact solutions in thick shell analysis.

2) Such an excellent agreement has been extended to the transverse shear and normal stresses. In contrast to other available modelings, such stresses are herein evaluate a priori, e.g., without implementing any postprocessing procedures.

3) An accurate a priori evaluation of transverse stresses requires a layerwise description.

4) In comparison to previous works related to flat geometries, thick shell problems require an accurate description of the curvature effects related to the radii to thickness ratio R/h. This fact has here been accounted for by extensive use of fictitious interfaces.

References

[1]Carrera, E., "Multilayered Shell Theories Accounting for Layerwise Mixed Description, Part 1: Governing Equations," *AIAA Journal*, Vol. 37, No. 9, 1999, pp. 1107–1116.

[2]Ren, J. G., "Exact Solutions for Laminated Cylindrical Shells in Cylindrical Bending," *Composite Science and Technology*, Vol. 29, 1987, pp. 169–187.

[3]Varadan, T. K., and Bhaskar, K., "Bending of Laminated Orthotropic Cylindrical Shells—An Elasticity Approach," *Composite Structures*, Vol. 17, 1991, pp. 141–156.

[4]Jing, H., and Tzeng, K., "Refined Shear Deformation Theory of Laminated Shells," *AIAA Journal*, Vol. 31, No. 4, 1993, pp. 765–773.

[5]Bhaskar, K., and Varadan, T. K., "Reissner's New Mixed Variational Principle Applied to Laminated Cylindrical Shells," *Journal of Pressure Vessel Technology*, Vol. 114, 1992, pp. 115–119.

[6]Carrera, E., "Evaluation of Layerwise Mixed Theories for Laminated Plates Analysis," *AIAA Journal*, Vol. 36, No. 5, 1998, pp. 830–839.

[7]Dennis, S. T., and Palazotto, A. N., "Laminated Shell in Cylindrical Bending, Two-Dimensional Approach vs Exact," *AIAA Journal*, Vol. 29, No. 4, 1991, pp. 647–650.

[8]Carrera, E., "Layer-Wise Mixed Models for Accurate Vibration Analysis of Multilayered Plates," *Journal of Applied Mechanics*, Vol. 65, 1998, pp. 820–824.

[9]Voyiadis, G. Z., and Shi, G., "A Refined Two-Dimensional Theory for Thick Cylindrical Shells," *International Journal of Solids and Structures*, Vol. 27, 1991, pp. 261–282.

[10]Noor, A. K., and Rarig, P. L., "Three-Dimensional Solutions of Laminated Cylinders," *Computer Method in Applied Mechanics and Engineering*, Vol. 3, 1974, pp. 319–334.

[11]Noor, A. K., and Peters, W. S., "Stress, Vibration and Buckling of Multilayered Cylinders," *Journal of Structural Engineering*, Vol. 115, 1989, pp. 69–89.

[12]Carrera, E., "C_z^0-Requirements: Models for the Two-Dimensional Analysis of Multilayered Structures," *Composite Structures*, Vol. 37, 1997, pp. 373–384.

[13]Murakami, H., "Laminated Composite Plate Theory with Improved In-Plane Response," *Journal of Applied Mechanics*, Vol. 53, 1986, pp. 661–666.

[14]Carrera, E., "C^0 Reissner-Mindlin Multilayered Plate Elements Including Zig-Zag and Interlaminar Stresses Continuity," *International Journal of Numerical Methods in Engineering*, Vol. 39, 1996, pp. 1797–1820.

[15]Librescu, L., Khdeir, A. A., and Frederick, D., "A Shear Deformable Theory of Laminated Composite Shallow Shell-Type Panels and Their Response Analysis. Part II: Static Response," *Acta Mechanica*, Vol. 77, 1989, pp. 1–12.

[16]Reddy, J. N., and Liu, C. F., "A Higher-Order Shear Deformation Theory of Laminated Elastic Shells," *International Journal of Engineering Sciences*, Vol. 23, 1985, pp. 319–330.

[17]Carrera, E., "A Class of Two Dimensional Theories for Multilayered Plates Analysis," *Atti Accademia delle Scienze di Torino, Mem. Sci. Fis.*, Vols. 19–20, 1995, pp. 49–87.

G. A. Kardomateas
Associate Editor